Journal of Engineering Mathematics **33:** 311–332, 1998.

On a stabilization procedure for the parabolic stability equations

P. ANDERSSON*, D. S. HENNINGSON* and A. HANIFI
Aeronautical Research Institute of Sweden (FFA), Box 11021, S-16111 Bromma, Sweden. e-mail: hnd@ffa.se

Received 4 June 1997; accepted in revised form 18 February 1998

Abstract. The numerical-stability consequences of the remaining ellipticity in the Parabolic Stability Equations (PSE) are studied. The analysis of Li and Malik of the constant-coefficient Navier-Stokes equations is extended by a detailed analysis of the parabolizing steps. Dropping of the highest streamwise derivative removes the slowest decaying upstream propagating mode, whereas the fastest remains. This mode can be numerically damped, by use of an implicit discretization of the streamwise derivative and a large enough streamwise step size. Suggestions of how to make the equations well-posed by the addition of a term proportional to the truncation error of the implicit scheme are given. This term is easy to implement, does not change the order of approximation and removes the step-size restriction. An explicit formula for the critical step size is also derived, in the modified equations, which shows that the equations are completely stabilized for a properly chosen stabilization parameter.

Keywords: parabolic stability equations, hydrodynamic stability, ill-posed equations, boundary-layer flow.

1. Introduction

In a variety of flow situations in fluid mechanics, the region where transition from laminar to turbulent flow takes place has to be determined. The most common transition-prediction methods are based on linear stability theory which describes the evolution of small disturbances. The classical stability theory is based on the assumption of parallel flow and does not account for either growth of the boundary layer or the upstream history of disturbances. In the framework of this theory, the equations of disturbance evolution are formulated in terms of an eigenvalue problem. The effects of growing boundary layers have been introduced into the stability theory by several authors, *e.g.* Gaster [1], Saric and Nayfeh [2], Gaponov [3] and El-Hady [4]. However, in these investigations the instability characteristics of disturbances were studied locally and the upstream history was not taken into account.

Recently, a nonlocal stability theory based on parabolized stability equations (PSE) has been developed. The fundamental assumption of this theory is that disturbances consist of a fast oscillatory part and an amplitude which varies slowly in the streamwise direction. The first to solve parabolic evolution equations for disturbances in the boundary layer was Hall [5], who considered steady Görtler vortices. Itoh [6] used a parabolic equation to study the evolution of small-amplitude Tollmien–Schlichting waves. The method was further developed by Herbert and Bertolotti [7, 8, 9, 10], who also derived the nonlinear parabolized stability equations. Simen and Dallmann [11, 12] independently developed a similar theory. Their contribution was to model consistently and generally convectively amplified waves with divergent or curved wave-rays and wave-fronts propagating in nonuniform flow.

The Parabolic Stability Equations share many features with the Parabolized Navier-Stokes (PNS) equations developed in the late sixties. One of the difficulties encountered in the Parab-

* Also at Department of Mechanics, KTH S-100 44 Stockholm, Sweden.

olized Navier-Stokes equations is the presence of the streamwise pressure gradient term, P_x, in the streamwise momentum equation, which permits information to be propagated upstream through subsonic portions of the flowfield such as a boundary layer (see Rubin [13] and Rubin and Tannehill [14]). As a consequence of this, a space-marching method of the solution is not well-posed and in many cases exponentially growing solutions (departure solutions) are encountered. Different methods have been suggested to avoid this problem; see Anderson *et al.* [15, pp. 433–440] for an extensively compiled review. Lubard and Helliwell [16] approximated P_x with a backward-difference formula. They found that, for step sizes $\Delta x > \Delta x_{\min}$, the calculations were stable and the departure effect was suppressed. Vigneron *et al.* [17, 18] extended Lubard and Helliwell's analysis, by treating P_x exactly in the supersonic region, but only keeping a fraction of P_x in the subsonic region. Other techniques for treating the equations numerically were proposed by, *e.g.* Lin and Rubin [19], Rubin and Lin [20] and Israeli and Lin [21].

The Parabolized Stability Equations, like the PNS equations, are not fully parabolic equations, see Haj-Hariri [22]. The remaining small ellipticity mainly comes from the gradient of the disturbance pressure. This makes it necessary to use an implicit scheme and a large enough marching step size in the streamwise direction to obtain a stable solution. If too small a step size is used, the solution will eventually diverge. Li and Malik [23, 24] showed that using the PSE-approximation on the constant coefficient two-dimensional Navier-Stokes equations leads to an ill-posed Cauchy problem. They also derived a distinct step-size restriction for this problem, valid when a first-order backward Euler scheme is used, similar to the step-size restriction encountered for the PNS. Furthermore, they showed that dropping the streamwise derivative of pressure in the primitive variable formulation, and the derivative of streamwise wavenumber in the stream-function formulation, reduces the step-size restriction considerably. However, the ellipticity cannot be completely removed, and dropping these terms affects solution accuracy for some flows, *e.g.* the rotating-disk flow.

In the present paper, the fundamental solutions of two-dimensional linearized Navier-Stokes equations for spatially developing disturbances are derived and compared to those of the parabolized stability equations. The parabolizing steps are analyzed and several examples of the step-size restriction are shown. Furthermore, a stabilizing procedure for PSE is suggested and successfully applied to several flow cases.

2. The spatial development of disturbances

2.1. The linearized two-dimensional navier-stokes equations

In order to study the effect of the PSE-approximation on the full elliptic equations, we first turn our attention towards the incompressible two-dimensional Navier-Stokes equations, which are linearized around a mean flow with streamwise velocity U and normal velocity V. We are interested in the spatial development of disturbances and Fourier-transform the disturbances in time. Since the equations are linear, it suffices to consider a single mode with fixed frequency ω. The non-dimensional disturbance equations are

$$u_x + v_y = 0, \tag{1a}$$

$$-i\omega u + Uu_x + U_x u + Vu_y + U_y v = -p_x + \frac{1}{R}(u_{xx} + u_{yy}), \tag{1b}$$

$$-i\omega v + U v_x + V_x u + V v_y + V_y v = -p_y + \frac{1}{R}(v_{xx} + v_{yy}), \tag{1c}$$

with boundary conditions

$$u = v = 0 \quad \text{at} \quad y = y_{\min} \quad \text{and} \quad y = y_{\max}.$$

where the first equation is the divergence-free constraint and the last two are the streamwise and normal momentum equations, respectively. Here x represents the streamwise and y the normal coordinate. Further, u and v are the velocity components of the disturbance in the x and y-directions, respectively; p is the disturbance pressure and $R = U_r L/\nu$ is the Reynolds number. Here U_r, L and ν denote the reference velocity, length and viscosity, respectively. Moreover, the indices $_x$ and $_y$ refer to the derivative with respect to the streamwise and normal direction, respectively.

Alternatively, Equation (1) can be written in terms of the stream function, ψ, defined as

$$u = \frac{\partial \psi}{\partial y}, \qquad v = -\frac{\partial \psi}{\partial x}.$$

Then, the resulting equation is

$$\left(-i\omega - \frac{1}{R}\nabla^2 + U\frac{\partial}{\partial x} + V\frac{\partial}{\partial y}\right)\nabla^2\psi - \nabla^2 U\frac{\partial \psi}{\partial x} - \nabla^2 V\frac{\partial \psi}{\partial y} = 0, \tag{2}$$

with

$$\nabla^2 = \frac{\partial^2}{\partial x^2} + \frac{\partial^2}{\partial y^2},$$

and with boundary conditions $\psi = \psi_y = 0$ at $y_{\min}$ and $y_{\max}$.

2.2. Parabolized stability equations

In this section the standard PSE-method will be applied to the system defined by Equation (1). The basic assumption in the derivation of the parabolic stability equations is that the streamwise variation of the mean flow is slow. We start the derivation of the parabolic stability equations by separating the disturbances into an amplitude function and an exponential function. For the streamwise component we have

$$\hat{u}(x, y) = \tilde{u}(x, y)\, \mathrm{e}^{i\int_{x_0}^{x} \alpha(\xi)\, \mathrm{d}\xi}, \tag{3}$$

where α is the complex streamwise wavenumber. Introducing the above *ansatz* into (1) we obtain the following system

$$\tilde{u}_x + i\alpha\tilde{u} + \tilde{v}_y = 0, \tag{4a}$$

$$-i\omega\tilde{u} + U\tilde{u}_x + i\alpha U\tilde{u} + U_x\tilde{u} + V\tilde{u}_y + U_y\tilde{v} = -\tilde{p}_x - i\alpha\tilde{p} + \frac{1}{R}\left(\tilde{u}_{xx} + 2i\alpha\tilde{u}_x + i\frac{\mathrm{d}\alpha}{\mathrm{d}x}\tilde{u} - \alpha^2\tilde{u} + \tilde{u}_{yy}a\right), \tag{4b}$$

$$-i\omega\tilde{v} + U\tilde{v}_x + i\alpha U\tilde{v} + V\tilde{v}_y + V_x\tilde{u} + V_y\tilde{v} = -\tilde{p}_y + \frac{1}{R}\left(\tilde{v}_{xx} + 2i\alpha\tilde{v}_x + i\frac{\mathrm{d}\alpha}{\mathrm{d}x}\tilde{v} - \alpha^2\tilde{v} + \tilde{v}_{yy}\right), \tag{4c}$$

with boundary conditions

$$\tilde{u} = \tilde{v} = 0, \qquad y = y_{\min} \quad \text{and} \quad y = y_{\max}.$$

To be consistent with the assumption of a slowly varying mean flow, we will assume that the amplitude functions, $\tilde{u}$, $\tilde{v}$ and $\tilde{p}$, and the wavenumber, α, are slowly varying functions of x. We assume

$$\frac{\partial}{\partial x}, \qquad V \sim O(R^{-1}),$$

while the sizes of other quantities are assumed to be of $O(1)$. Neglecting all terms of order $O(R^{-2})$ and higher, we arrive at the following system of equations

$$\tilde{\mathbf{q}}_x = \mathcal{L}\tilde{\mathbf{q}}, \tag{5}$$

where

$$\mathcal{L} = \begin{bmatrix} -i\alpha & -D & 0 \\ 0 & -\dfrac{c_1}{U} - \dfrac{V_y}{U} & -\dfrac{D}{U} \\ -c_1 + i\alpha U - U_x & UD - U_y & -i\alpha \end{bmatrix} \tag{6}$$

$$\mathbf{q} = (u,\ v,\ p)^T, \qquad c_1 = i\alpha U - i\omega + VD - \frac{1}{R}(D^2 - \alpha^2)$$

and with boundary conditions $\tilde{u} = \tilde{v} = 0$ at $y = y_{\min}$ and $y = y_{\max}$. Here, D denotes the derivative with respect to the normal direction, y, and superscript ^{T} refers to the transpose of the vector. Notice that no second-order x-derivatives are left in the equations. To remove the ambiguity in expression (3), both the amplitude functions and the streamwise wavenumber are assumed to be functions of x, the auxiliary condition

$$\int_{y_{\min}}^{y_{\max}} (\tilde{u}^*\tilde{u}_x + \tilde{v}^*\tilde{v}_x + \tilde{p}^*\tilde{p}_x)\, \mathrm{d}y = 0, \tag{7}$$

can be used. This relation ensures that most of the x-variation of the disturbances will find its way into the exponential function and the streamwise variation of $\tilde{\mathbf{q}}$ remains small, in accordance with our original assumption. We solve Equations (5) by marching downstream, starting with an appropriate initial condition.

The corresponding stream-function formulation of Equations (5) is

$$(\mathcal{L}_0 + \mathcal{L}_1)\tilde{\psi} + \mathcal{L}_2\tilde{\psi}_x + i\frac{\mathrm{d}\alpha}{\mathrm{d}x}\mathcal{L}_3\tilde{\psi} = 0, \tag{8}$$

with boundary conditions $\tilde{\psi} = \tilde{\psi}_y = 0$ at $y_{\min}$ and $y_{\max}$. The operators $\mathcal{L}_0$ to $\mathcal{L}_3$ operate only in y and are

$$\mathcal{L}_0 = -\frac{1}{R}(D^2 - \alpha^2)^2 + (i\alpha U - i\omega)(D^2 - \alpha^2) - i\alpha U_{yy},$$

$$\mathcal{L}_1 = -V_{yy}D + V(D^2 - \alpha^2)D,$$

$$\mathcal{L}_2 = U(D^2 - 3\alpha^2) + 2\alpha\omega - U_{yy},$$

$$\mathcal{L}_3 = -i\omega + 3i\alpha U.$$

The auxiliary condition can be formulated as

$$\int_{y_{\min}}^{y_{\max}} \tilde{\psi}^* \tilde{\psi}_x \, \mathrm{d}y = 0. \tag{9}$$

3. Fundamental solutions to the constant-coefficient problem

3.1. Two-dimensional Navier-Stokes equations

To simplify the theoretical studies, we apply a Fourier transform of the disturbance quantities in the y-direction. We use η to denote the wavenumber in this direction. We start with the two-dimensional Navier-Stokes Equations (1a–c) and find,

$$\hat{u}_x + i\eta\hat{v} = 0, \tag{10a}$$

$$-i\omega\hat{u} + U\hat{u}_x + U_x\hat{u} + i\eta V\hat{u} + U_y\hat{v} = -\hat{p}_x + \frac{1}{R}(\hat{u}_{xx} - \eta^2\hat{u}), \tag{10b}$$

$$-i\omega\hat{v} + U\hat{v}_x + V_x\hat{u} + i\eta V\hat{v} + V_y\hat{v} = -i\eta\hat{p} + \frac{1}{R}(\hat{v}_{xx} - \eta^2\hat{v}), \tag{10c}$$

where the superscript $\hat{}$ refers to Fourier-transformed quantities. Here we will consider the fundamental solutions to the system of Equations (10). For simplicity, we restrict ourselves to a constant mean flow. To compare the exact solutions of the complete equations to those obtained by means of the PSE-approximation, we assume the solutions to be of the form

$$\hat{\mathbf{q}}(x) = \tilde{\mathbf{q}}(x)\, \mathrm{e}^{\,i\int_{x_0}^{x}\alpha(\xi)\,\mathrm{d}\xi}. \tag{11}$$

Introducing the above *ansatz* into the disturbance Equations (10), we obtain the system

$$\frac{\mathrm{d}}{\mathrm{d}x}\begin{pmatrix}\tilde{u}\\ \tilde{v}\\ \tilde{v}_x\\ \tilde{p}\end{pmatrix} = \begin{bmatrix} -i\alpha & -i\eta & 0 & 0\\ 0 & -i\alpha & 1 & 0\\ 0 & c_2 & UR - i\alpha & i\eta R\\ c_3 & i\eta U & -i\dfrac{\eta}{R} & -i\alpha \end{bmatrix}\begin{pmatrix}\tilde{u}\\ \tilde{v}\\ \tilde{v}_x\\ \tilde{p}\end{pmatrix}, \tag{12}$$

where

$$c_2 = (-i\omega + i\eta V)R + \eta^2, \qquad c_3 = i\omega - i\eta V - \frac{\eta^2}{R}.$$

Here, we have eliminated the $\hat{u}_{xx}$-term, using the x-derivative of the continuity equation. The solutions to the system above can be constructed formally from the eigenvalues and eigenvectors of the matrix representing the evolution operator.

The eigenvalues, λ_i, and their corresponding eigenvectors, Φ_i, of system (12) are,

$$\lambda_{1,2} = -i\alpha \pm \eta, \tag{13a}$$

$$\lambda_{3,4} = -i\alpha + \frac{UR}{2} \pm \frac{1}{2}\sqrt{U^2R^2 + 4\eta^2 + 4iV\eta R - 4i\omega R}, \tag{13b}$$

and

$$\Phi_1 = (i,\ 1,\ \lambda_1,\ \frac{\omega}{\eta} - V - iU)^T, \tag{14a}$$

$$\Phi_2 = (-i,\ 1,\ \lambda_2,\ \frac{\omega}{\eta} - V + iU)^T, \tag{14b}$$

$$\Phi_3 = (\eta,\ i\lambda_3 - \alpha,\ \lambda_3[i\lambda_3 - \alpha],\ 0)^T, \tag{14c}$$

$$\Phi_4 = (\eta,\ i\lambda_4 - \alpha,\ \lambda_4[i\lambda_4 - \alpha],\ 0)^T. \tag{14d}$$

A characteristic feature of a parabolic system is that the information propagates in one direction only. This makes it possible for us to calculate the solution to such a system by marching in the propagation direction. The propagation directions of the eigenmodes are given by their group velocities defined as

$$C_g = \frac{\partial\omega}{\partial\alpha}.$$

The group velocities can be obtained by differentiation of the expressions for the eigenvalues, λ,

$$\frac{\partial\lambda}{\partial\alpha}\,\mathrm{d}\alpha + \frac{\partial\lambda}{\partial\omega}\,\mathrm{d}\omega = 0, \tag{15}$$

which gives,

$$\frac{\mathrm{d}\omega}{\mathrm{d}\alpha} = -\frac{\partial\lambda}{\partial\alpha}\Big/\frac{\partial\lambda}{\partial\omega}. \tag{16}$$

The first two eigenvalues, $\lambda_{1,2}$, are associated with the disturbance pressure. Since these eigenvalues are independent of ω, the corresponding group velocities can be thought of as infinite, one traveling upstream and the other downstream. A Taylor-series expansion of $\lambda_{3,4}$, for large UR, gives

$$\lambda_3 \approx -i\alpha + UR + \frac{\eta^2}{UR} + \frac{i\eta V}{U} - \frac{i\omega}{U}, \tag{17a}$$

$$\lambda_4 \approx -i\alpha - \frac{\eta^2}{UR} - \frac{i\eta V}{U} + \frac{i\omega}{U}, \tag{17b}$$

which yields

$$C_{g3} \approx -U, \qquad C_{g4} \approx U. \tag{18}$$

The above expressions imply that λ_3 and λ_4 correspond to up- and downstream traveling solutions, respectively. In order to obtain a set of equations of a parabolic nature, the two eigenvalues associated with upstream propagating disturbances must be removed or suppressed. In fact, to extract just the solution which is relevant, it is necessary to suppress solutions associated with all eigenvalues, except λ_4.

Of course, the fundamental solutions to a system of equations do not change when we rewrite them in another form. Therefore, the eigenvalues to the stream-function-formulated equations become exactly the same as for the primitive variable formulation. So, the same eigenmodes appear, which have to be removed in order to get parabolic equations. However, we will see in Sections 3.2 and 5.1 that, due to the nature of the numerical instability, it can be preferable to use the PSE-approximated stream-function formulation, rather than the primitive-variable formulation, when this is possible. Note that the stream-function formulation can only be used for two-dimensional flow.

3.2. PARABOLIZED STABILITY EQUATIONS

The assumption of periodicity in the normal direction reduces the operator $\mathcal{L}$ in Equation (6) to

$$\mathcal{L} = \begin{bmatrix} -i\alpha & -i\eta & 0 \\ 0 & -\dfrac{c_4}{U} - \dfrac{V_y}{U} & -\dfrac{i\eta}{U} \\ -c_4 + i\alpha U - U_x & i\eta U - U_y & -i\alpha \end{bmatrix}, \tag{19}$$

where

$$c_4 = i\alpha U - i\omega + i\eta V + \frac{\alpha^2}{R} + \frac{\eta^2}{R}.$$

Now, let us consider the constant-coefficient case, *i.e.* $U_x = U_y = V_x = V_y = 0$. Performing the same analysis as in the previous subsection, we obtain the eigenvalues and eigenvectors as

$$\kappa_{1,2} = -i\alpha \pm \eta, \qquad \kappa_3 = -i\alpha + \frac{i\omega}{U} - \frac{i\eta V}{U} - \frac{\eta^2}{UR} - \frac{\alpha^2}{UR}, \tag{20}$$

and

$$\Omega_{1,2} = \left(1,\ \pm i,\ \pm\frac{i\alpha U - c_4}{\eta} - U\right)^T, \qquad \Omega_3 = \left(1,\ -\frac{U\alpha + ic_4}{U\eta},\ 0\right)^T. \tag{21}$$

These eigenvalues and eigenvectors can be compared to those shown in (13) and (14). We see directly that the first two eigenvalues, $\kappa_{1,2}$, are identical to $\lambda_{1,2}$. The group velocity corresponding to the third eigenvalue, κ_3, is, to leading order, given by

$$C_{g3} \approx U. \tag{22}$$

This is, to leading order, the group velocity of the fourth eigenvalue of the two-dimensional Navier-Stokes equations (see Equations (17)). This implies that the parabolization procedure

done in the PSE-approach eliminates one of the upstream propagating eigenmodes, namely the one with group velocity $-U$, but leaves the one associated with the upstream propagation of pressure disturbances. As will be shown later, the existence of eigenmodes corresponding to the eigenvalues κ_1 and κ_2, causes a numerical instability which prevents us from taking arbitrarily small step sizes when the solution is marched in the streamwise direction.

In the stream-function-formulated PSEs, the evolution operator becomes a scalar. We apply the PSE-approximation to Equation (8). Let us now apply a Fourier transform in the normal direction and consider the constant-coefficient case. Then, the eigenvalue associated with the evolution operator becomes

$$-\frac{(\eta^2+\alpha^2)c_4}{U(\eta^2+3\alpha^2)-2\alpha\omega}. \tag{23}$$

Since there is only one eigenvalue, there are no extra eigenmodes to damp out in the marching procedure, indicating a less severe step-size restriction. However, we should remember that α is not known *a priori* in the calculations.

4. Simple example of the step-size problem

Here, we demonstrate the numerical-instability problem of the PSE-approximation by solving the equations for a one-dimensional basic flow with disturbances which are periodic in the normal direction. We also restrict ourselves to a parallel mean flow with,

$$V=0, \quad U=\begin{cases} 0{\cdot}5; & 0\leqslant x\leqslant 0{\cdot}4; \\ -125x^3+187{\cdot}5x^2-90x+14{\cdot}5; & 0{\cdot}4<x<0{\cdot}6; \\ 1; & 0{\cdot}6\leqslant x\leqslant 1. \end{cases}$$

The mean flow is plotted in Figure 1a. The auxiliary condition now becomes

$$\tilde{u}^*\tilde{u}_x+\tilde{v}^*\tilde{v}_x+\tilde{p}^*\tilde{p}_x=0.$$

Here, we solved Equations (5) numerically by discretizing the x-derivative of the 3×3-system with a first-order backward Euler scheme. A secant method was used to find α such that the auxiliary condition was fulfilled. Moreover, we found the initial conditions by solving the local x-independent system.

The system of equations was solved with the mean field given above and the flow parameters $R=10^5$, $\omega=100$ and $\eta=100$. In Figures 1c and 1d the growth rates of the disturbances, $\hat{u}$ and $\hat{v}$ are given. The growth rate for the $\hat{u}$ component is defined as

$$-\alpha_i+\Re e\left\{\frac{\mathrm{d}}{\mathrm{d}x}\log(\tilde{u})\right\},$$

and similar for the $\hat{v}$ component of the disturbance. For comparison, the results obtained from the local theory and the multiple-scales method are also given there. The details of the multiple-scales method are discussed in Appendix 7. The PSE results showed an oscillatory behavior for $x>0{\cdot}55$. These oscillations increased with decreasing step size, Δx. For $\Delta x=0{\cdot}0093$, the calculations started to diverge. As is demonstrated in these figures, converged

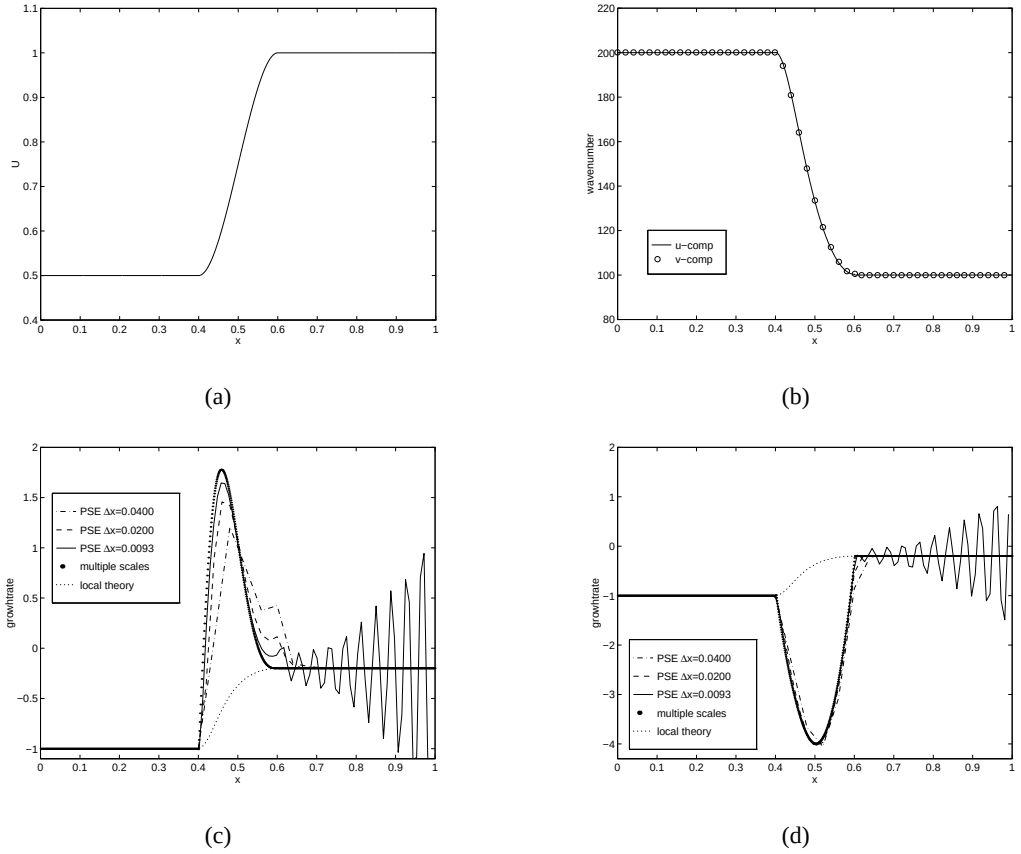

(a) (b)

(c) (d)

Figure 1. (a) Step function describing the mean field, (b) streamwise wavenumber *vs* streamwise position for the $\hat{u}$ and $\hat{v}$ components. Growth rate *vs* streamwise position for the (c) $\hat{u}$ (d) $\hat{v}$ component calculated with PSE-method, multiple-scales method and local theory.

stable solution could not be obtained here. The large difference between the local and non-local theories, in the region where the mean flow varies, shows the importance of incorporating non-parallel effects in the theory.

Furthermore, it should be noted that the oscillations started at the position where $\Delta x < 1/|\alpha_r|$, as was suggested by Li and Malik [23, 24] (see Figure 1b).

It should be mentioned here that the variation of the mean flow is rapid and some of the basic assumptions may not be valid. However, the PSE-results approach those of the multiple scales. This illustrates that there are cases where a converged solution cannot be found before the instability associated with the small step sizes occurs. The existence of such cases motivates a study with the aim to stabilize the PSEs and to remove the step-size restriction.

5. Stabilization of the PSE-equations

5.1. Well-posedness of the PSE

Well-posedness is an important instrument in numerical analysis to decide whether it is worthwhile to try and solve an equation numerically. Usually, ill-posedness of the equations means

that any attempt to solve them numerically is fruitless, since the solution will always start to grow without bound at some point in the calculation domain. Once we know that the equations are well-posed, a stable numerical scheme can be chosen to obtain a numerical solution that converges to the analytical one.

Well-posedness, in the Kreiss and Lorenz sense [25, pp. 23–80], means that the solution is permitted to grow at most exponentially. Mathematically, this means that

$$|e^{\kappa_i x}| \leqslant K e^{\gamma x}, \tag{24}$$

where K and γ are constants and κ_i are all the eigenvalues of the constant-coefficient spatial operator. For the first two eigenvalues PSE-system, which are κ_1 and κ_2 as given in Equations (20), we have

$$|e^{(-i\alpha\pm\eta)x}| \to \infty, \quad \text{when } \eta \to \pm\infty, \tag{25}$$

which means that the solution can grow without bound when η approaches infinity. This implies that the equations are ill-posed. In the following section it will be shown how we may overcome this by choosing a numerical algorithm that damps out the solutions corresponding to these two eigenvalues, leaving the solution that corresponds to the third eigenvalue, which is the solution of interest.

The stream-function formulation reduces the spatial operator to a scalar, see (23). The real part of this scalar stays negative when $|\eta| \to \infty$, for reasonable values of the flow parameters. This means that, in terms of well-posedness, the stream-function-formulated PSEs are well-posed in the Kreiss and Lorenz sense. This indicates that we may expect a less severe step-size restriction than was needed for the primitive-variable-formulated equations, as found *e.g.* by Li and Malik [24].

5.2. Stabilization by means of a backward Euler scheme

In the preceding sections we have shown that the PSE-approximation removes one of the eigenvalues that corresponds to an upstream propagating mode. It has also been seen that the first two eigenvalues κ_1 and κ_2 are responsible for making the equations ill-posed. In this section it will be shown that it is possible to damp out these two eigenvalues numerically. The argument follows that of Li and Malik [23, 24], and is given here for completeness.

Since the eigenvalues are distinct, we can write Equations (5), with constant coefficients, as three separable equations

$$\frac{d\phi_i}{dx} = \kappa_i \phi_i. \tag{26}$$

Here κ_1, κ_2 and κ_3 are the three eigenvalues of the matrix operator in (19), as given in (20). Moreover, ϕ_1, ϕ_2 and ϕ_3 contain an appropriate linear combination of $\tilde{u}$, $\tilde{v}$ and $\tilde{p}$. Applying the first-order backward Euler scheme, we have

$$\phi^{n+1} = \frac{\phi^n}{1 - \Delta x \kappa_i} = \gamma_i \phi^n. \tag{27}$$

Here, γ_i is called the amplification factor. To obtain absolute stability of the numerical scheme, the condition $|\gamma_i| < 1$ must hold for all κ_i. Introducing κ_1 and κ_2 into the expression for the amplification factor, we find

$$\gamma_{1,2} = \frac{1}{[1 + (\alpha_i \pm \eta)\Delta x] + i\alpha_r \Delta x}, \tag{28}$$

where α_r and α_i are the real and imaginary parts of α, respectively. Since η can take any value on the real axis, the only way to ensure that $|\gamma_{1,2}| < 1$ holds is to make sure that the inequality

$$\Delta x > \frac{1}{|\alpha_r|}, \tag{29}$$

is valid for all values of η. The above step-size restriction seems to hold for most PSE applications. It is easy to show that an explicit scheme will always produce numerical instabilities. Thus, a crucial part of the PSE method is to use an implicit scheme with a large enough step size in the streamwise direction.

5.3. Stabilization by addition of a truncation error

5.3.1. *Stabilized equations*

It is unsatisfactory to work with ill-posed equations. Therefore, in this section we shall make suggestions on how to stabilize the PSEs for arbitrarily small step sizes. The goal is to modify the system of equations such that the numerical instability is removed, but the physical solutions remain unchanged.

The truncation error to the first-order backward Euler scheme becomes

$$\tau = \frac{\Delta x}{2}\tilde{\mathbf{q}}_{xx} + \cdots$$

Since we have assumed that the streamwise variation of the amplitude function is of order $O(R^{-1})$, the terms signified by $\cdots$ in the expression above will be of order $O(R^{-3}\Delta x^2)$. Dropping all but the leading terms of the truncation error and using Equation (5), we get

$$\tau = \frac{\Delta x}{2}\tilde{\mathbf{q}}_{xx} = \frac{\Delta x}{2}(\mathcal{L}_x\tilde{\mathbf{q}} + \mathcal{L}\tilde{\mathbf{q}}_x) \approx \frac{\Delta x}{2}\mathcal{L}\tilde{\mathbf{q}}_x, \tag{30}$$

Here, the term $\mathcal{L}_x\tilde{\mathbf{q}}$ has been neglected for simplicity. However, equality holds if $\mathcal{L}$ is independent of x. Recall that the assumption of small x-derivative terms implies that the added truncation error is of the order $O(R^{-2})$. Since terms of this order were neglected in the original approximation, the addition of τ does not introduce any extra error at this order of approximation, and we can introduce the new set of equations

$$\tilde{\mathbf{q}}_x = \mathcal{L}\tilde{\mathbf{q}} + s\mathcal{L}\tilde{\mathbf{q}}_x. \tag{31}$$

Here, s is a positive real number. Based on the discussion given above, the differences between the solution of Equations (5) and (31) are of order $O(R^{-2})$. Note that, although s take the place of Δx in the added truncation error term, this term is small, even if $s = O(1)$, since $\mathcal{L}\tilde{\mathbf{q}}_x$ was shown to be of order $O(R^{-2})$.

As was mentioned before, the PSE method includes an iteration to fulfill the auxiliary condition, where α is iterated until the auxiliary condition is fulfilled. Based on the auxiliary condition, we can introduce the norm

$$\int_{y_{\min}}^{y_{\max}} \tilde{\mathbf{q}}^\dagger\tilde{\mathbf{q}}_x \, \mathrm{d}y = (\tilde{\mathbf{q}}, \tilde{\mathbf{q}}_x),$$

where † denotes the complex conjugate. In the original case, this gives the equation

$$(\tilde{\mathbf{q}}, \tilde{\mathbf{q}}_x) = (\tilde{\mathbf{q}}, \mathcal{L}\tilde{\mathbf{q}}) = 0,$$

to which we have to apply an iteration procedure to obtain α. In the modified case we get

$$(\tilde{\mathbf{q}}, \tilde{\mathbf{q}}_x) = (\tilde{\mathbf{q}}, \mathcal{L}\tilde{\mathbf{q}}) + s(\tilde{\mathbf{q}}, \mathcal{L}\tilde{\mathbf{q}}_x) = 0.$$

We find that the additional term in the equation for α also is of the order $O(R^{-2})$, implying formally that the difference in α values will be of the same order as those terms that were originally neglected in the PSE approximation. Thus, added terms do not contribute any extra error at the given order of approximation in inverse powers of the Reynolds number. However, if the streamwise variation of the amplitude function becomes rapid, the error may become significant.

In the following the numerical instability of Equation (31) will be examined and its efficiency in removing the step-size problem will be demonstrated.

5.3.2. *Stability analysis of the modified equations*

Here we will study the numerical stability of the Equations (5), modified by the term $s\mathcal{L}\tilde{\mathbf{q}}_x$. We recall the operator $\mathcal{L}$ of Equation (19) and consider the constant-coefficients case. Then, the eigenvalues of Equation (31) become

$$\kappa_1^S = \frac{\kappa_1}{1 - s\kappa_1}, \qquad \kappa_2^S = \frac{\kappa_2}{1 - s\kappa_2}, \qquad \kappa_3^S = \frac{\kappa_3}{1 - s\kappa_3}, \tag{32}$$

where κ_1, κ_2 and κ_3 are the eigenvalues of the original system, given in Equations (20). The eigenvectors remain the same as those of $\mathcal{L}$, given in Equations (21).

Let us repeat the analysis of Section 5.2 for the modified PSEs. Using first-order backward Euler, we find that the discretized form of Equation (31) reads

$$(I - \Delta x\mathcal{L} - s\mathcal{L})\tilde{\mathbf{q}}^{n+1} = (I - s\mathcal{L})\tilde{\mathbf{q}}^n, \tag{33}$$

which gives the amplification factors

$$\gamma_i = \frac{1 - s\kappa_i}{1 - (\Delta x + s)\kappa_i}.$$

For absolute stability we demand $|\gamma_i| < 1$ for all values of η. The two troublesome eigenmodes become

$$|\gamma_{1,2}|^2 = \left|\frac{1 - s\kappa_{1,2}}{1 - (\Delta x + s)\kappa_{1,2}}\right|^2 = \frac{[1 - s(\alpha_i \pm \eta)]^2 + (s\alpha_r)^2}{[1 - (\Delta x + s)(\alpha_i \pm \eta)]^2 + [(\Delta x + s)\alpha_r]^2}.$$

The condition

$$\max_{\eta} |\gamma_{1,2}|^2 < 1,$$

gives the critical step size as

$$\Delta x > \frac{1}{|\alpha_r|} - 2s. \tag{34}$$

We performed the maximization in a standard manner by taking derivatives and searching for extrema. Equation (34) implies that the s value giving marginal stability approaches $0{\cdot}5/|\alpha_r|$ when $\Delta x \to 0$. Consequently, we can stably march PSEs downstream for any arbitrarily small step size by using a suitable s.

5.3.3. *Well-posedness of the modified equations*
The eigenvalues to the modified system are

$$\kappa_{1,2}^S = \frac{-i\alpha \pm \eta}{1 - s(-i\alpha \pm \eta)}, \qquad \kappa_3^S = -\frac{c_5}{U + sc_5}, \tag{35}$$

where

$$c_5 = i\alpha U - i\omega + i\eta V + \frac{\alpha^2}{R} + \frac{\eta^2}{R}.$$

It is evident that the first two eigenvalues approach $-1/s$ when $\eta \to \pm\infty$ and, as long as $\alpha_r \neq 0$, these eigenvalues will have finite maxima. The same argument is true for the third eigenvalue, for reasonable values of the flow parameters. If all eigenvalues contain a maximum value for some η, it is possible to find constants K and γ such that

$$|\mathrm{e}^{\kappa_i^S x}| \leqslant K\mathrm{e}^{\gamma x} \tag{36}$$

holds for all values of η. Recalling the definition of well-posedness, we can conclude that the new system of equations is well-posed.

6. Numerical examples of the stabilizing procedure

In order to demonstrate the efficiency of the suggested stabilizing procedure, we solved the stabilized PSEs for different basic flows. A comparison between these results and those from the original PSEs are given below.

6.1. y-PERIODIC DISTURBANCES REVISITED

We added a term proportional to the truncation error of the backward Euler scheme to the Fourier-transformed problem from Section 4. The new system of equations was discretized in the same fashion as the original PSE-system. The stabilizing parameter s was set to $s = 1$. From Equation (34) we get the critical value of s as $s = 0{\cdot}0049$, for which an arbitrary small step size can be used. Despite the rapid variation of the mean flow which contrasts with our basic assumptions, the results were found to be in good agreement with those obtained from the method of multiple scales. Furthermore, numerical instability was not observed for small step sizes. Thus, for these flow parameters, the stabilization procedure allowed us to obtain a converged solution, which could not be obtained with the original PSE formulation. The results for a step size $\Delta x = 2 \times 10^{-4}$, *i.e.* well below the previously found step-size restriction limit of $\Delta x \approx 0{\cdot}01$, are given in Figure 2. The growth rate from the method of multiple scales is also plotted there.

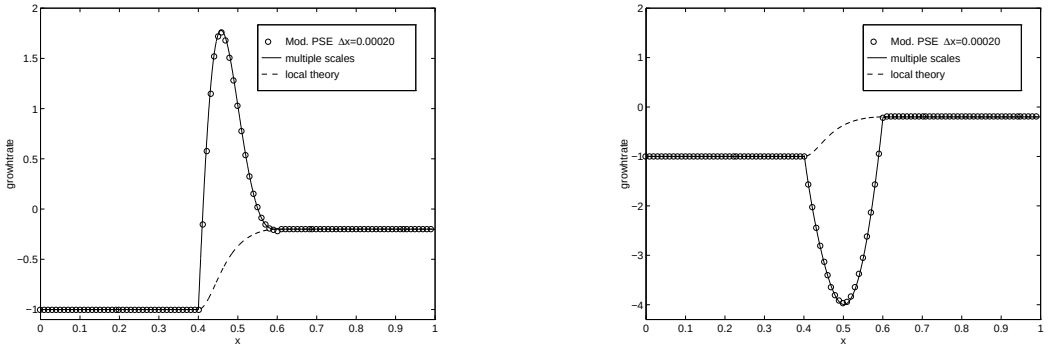

(a) (b)

Figure 2. Growth rate *vs* streamwise position, for y-periodic disturbances, with stabilizing terms for the (a) $\hat{u}$ (b) $\hat{v}$ component calculated with PSE method, multiple-scales method and local theory.

6.2. BOUNDARY-LAYER FLOW

The stabilizing procedure was also successfully applied to a non-parallel boundary-layer flow. The equations were linearized around the two-dimensional Blasius boundary-layer flow, *i.e.* the solution to the equation

$$ff'' + 2f''' = 0, \tag{37}$$

where,

$$U^*(x, y) = U_\infty f'(\xi), \qquad V^*(x, y) = \frac{1}{2}\sqrt{\frac{\nu U_\infty}{x^*}}(\xi f'(\xi) - f(\xi)), \tag{38}$$

with

$$\xi = y^*\sqrt{\frac{U_\infty}{\nu x^*}},$$

and boundary conditions

$$\xi = 0 : f = 0, \quad f' = 0, \qquad \xi \to \infty : f' \to 1.$$

The disturbances were governed by Equations (5) and subjected to the boundary conditions

$$y = 0 : u = v = 0; \qquad y \to \infty : u,\ v,\ p \to 0.$$

The calculations where made for the same case as studied by Li and Malik [23, 24], with a disturbance frequency $F = 70 \times 10^{-6}$, where

$$F = \frac{2\pi\nu}{U_\infty^2} f^*,$$

with f^* being the physical frequency. The calculations were started at $R = U_\infty L/\nu = 500$, where $L = \sqrt{\nu x_0^*/U_\infty}$. Dimensional variables are denoted by * for these parameters. The

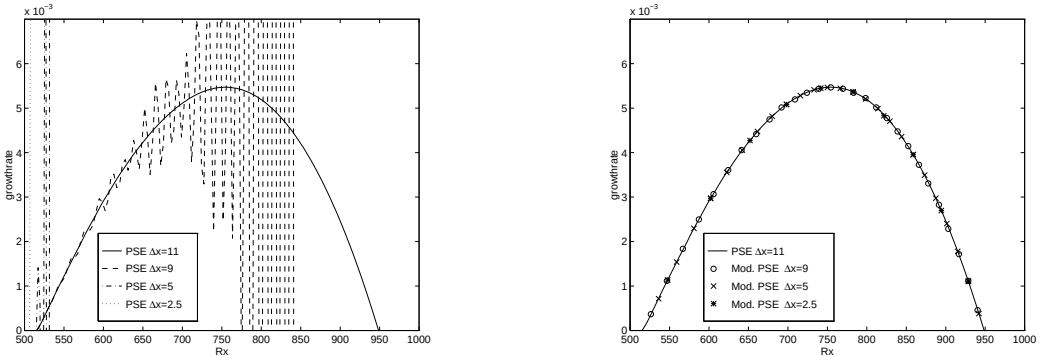

(a) (b)

Figure 3. Growth rate *vs* streamwise position, for boundary-layer flow, obtained from the PSE method without (a) with (b) stabilizing terms for the three smallest step sizes. The value of the stabilizing parameter was set to $s = 4$.

real part of the streamwise wavenumber was $\alpha_r \approx 0{\cdot}106$, which gave a critical step size of approximately $\Delta x = 9{\cdot}5$ based on the length scale at $R = 500$. The calculations were performed for four different step sizes $\Delta x = 11$, 9, 5 and $2{\cdot}5$. In Figure 3a the results for the original PSEs are presented. Here the growth rate was based on the maximum of $\tilde{u}$, *i.e.*

$$-\alpha_i + \Re e \left\{ \frac{\mathrm{d}}{\mathrm{d}x} \log(\tilde{u}_{\max}) \right\}.$$

As can be seen there, we only obtained a smooth solution for the stable step size, $\Delta x = 11$. All attempts to march with step sizes under the critical value became numerically unstable at some point in the calculation domain.

The results from the modified PSEs with $s = 4$ are given in Figure 3b. The disturbance growth rate calculated from the original PSEs for $\Delta x = 11$ is also given for reference purposes. As is shown there, numerical instability was absent in these calculations and results for all step sizes collapsed to the same curve.

To investigate the effect of the parameter s on the results and to test the step-size restriction given by Equation (34) for the modified equations, we calculated the growth rate using a step size smaller than the critical value for the original PSEs, $\Delta x = 5$. Three different values of the parameter s were used, one just under $s = 2$, one just over $s = 2{\cdot}5$ and one considerably larger $s = 10$ than the critical value $s \approx 2{\cdot}1$. All flow parameters were identical to those used to obtain the results in Figures 3a and 3b. The results are presented in Figure 4a together with the results of the original PSEs with $\Delta x = 11$ for reference purposes. These results show that, if the parameter s is larger than its critical value, it does not affect the results, but removes the numerical instability. However, the instability is still present for those values of s which are smaller than the critical value.

To further test the step-size restriction for the modified PSEs, we repeated the calculations for the different values of Δx and s plotted in Figure 4c. When using combinations of $(\Delta x, s)$ in the stable region, we obtained converged solutions. However, all attempts to march with combinations of $(\Delta x, s)$ in the unstable region gave numerical instabilities (see Figures 4a–c).

Li and Malik [23, 24] stabilize the equations by putting $\partial \tilde{p}/\partial x = 0$, a strategy which is sometimes used for the solution of the PNS equations. This does not introduce any visual

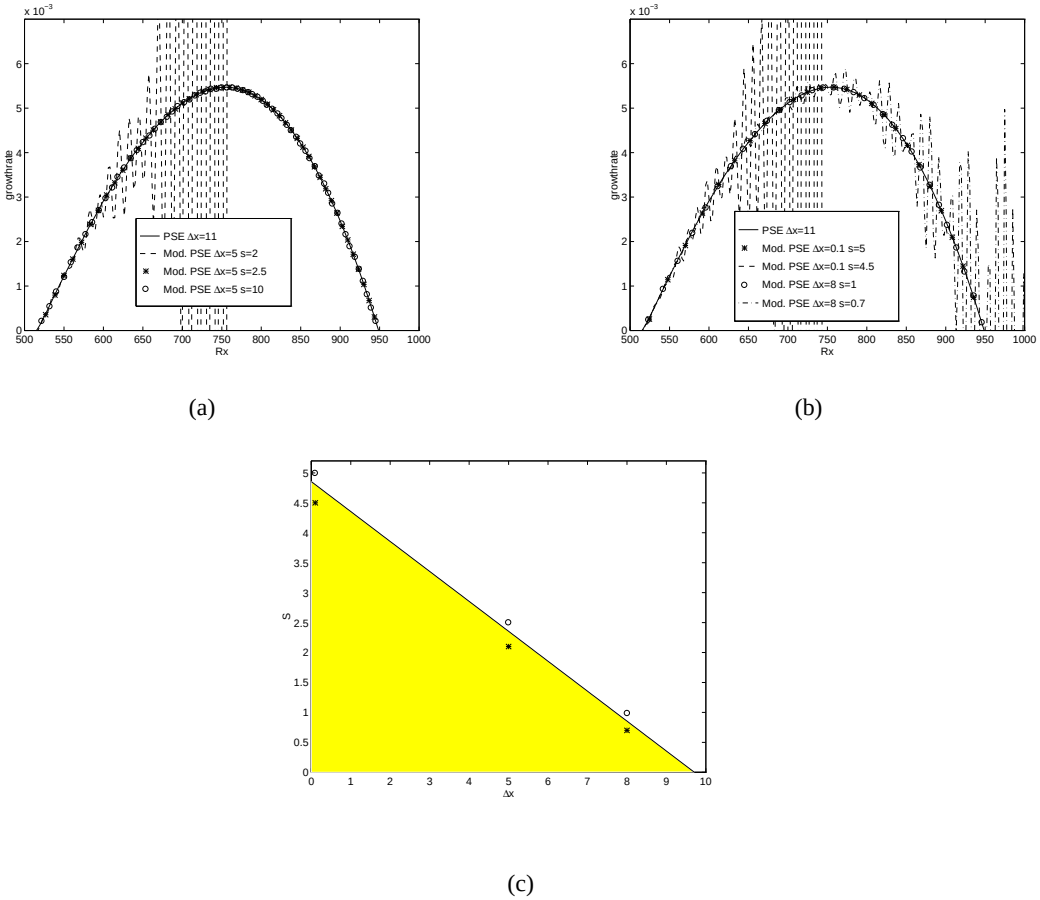

Figure 4. Solutions of the modified PSEs, in the Blasius boundary layer, for different values of the stabilizing parameter s and the step size Δx. (a) Growth rate *vs* streamwise position. (b) Growth rate *vs* streamwise position (c) Combinations of $(\Delta x, s)$ corresponding to stable or unstable marching conditions. Circles(stars) correspond to stable(unstable) solutions in Figures 4a and 4b. Note that the line is given by Equation (34) derived in Section 5.3.2.

error for the Blasius boundary-layer case studied here (see, however, the rotating-disk flow in Section 6.3). Dropping of the $\partial \tilde{p}/\partial x$-term makes it possible to march the equations with a smaller streamwise step size. However, the solution blows up when the step size $\Delta x = 0{\cdot}25$ is used and numerical instabilities occur earlier for the smaller step size $\Delta x = 0{\cdot}2$.

6.3. Flow near a rotating disk

We now consider the three-dimensional flow over an infinite rotating disk. The equations are written in (r, θ, y) coordinates, where r is the radius from the rotating axis, θ is the azimuthal coordinate, and y the height above the disk. The von Karman solution is used as mean flow, *i.e.*

$$F^2 - (G+1)^2 + F'H - F'' = 0,$$

$$2F(G+1) + G'H - G'' = 0,$$

$$2F + H' = 0,$$

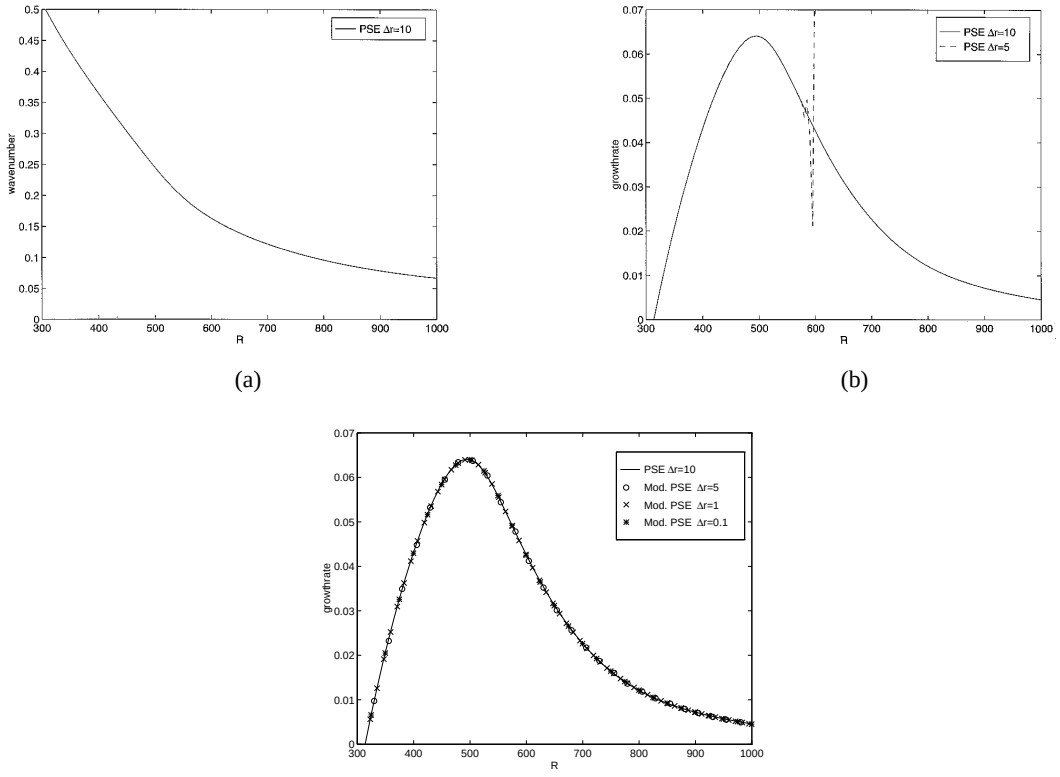

Figure 5. Rotating-disk flow. (a) Streamwise wavenumber *vs* streamwise position, and growth rate *vs* streamwise position as obtained from the PSE method without (b) with (c) stabilizing terms for the three smallest step sizes.

where

$$U(r, y) = rF(y), \qquad W(r, y) = rG(y), \qquad V(y) = H(y),$$

and with the boundary conditions

$$y = 0 : F = G = H = 0; \qquad y \to \infty : F \to 0,\ G \to -1.$$

Here U, V, and W are the non-dimensional velocity components in the r, y and θ directions, respectively. The reference length is taken as $L = \sqrt{\nu/\Omega^*}$ and reference velocity $U_{\text{ref}} = \sqrt{\nu\Omega^*}$, where Ω^* is the dimensional angular velocity of the rotating disk. The Reynolds number at position r^* is defined as $R = r^*\sqrt{\Omega^*/\nu}$. Here * refers to dimensional variables. The equations that we solve are given in Appendix B.

The calculations were made for a case which is identical to that studied by Li and Malik [24]. They considered stationary cross-flow disturbances, *i.e.* $\omega = 0$, with the azimuthal number of waves $n = 30$. The growth rate is based on the maximum of the azimuthal disturbance velocity $\tilde{w}$, *i.e.*

$$-\alpha_i + \Re e\left\{\frac{\mathrm{d}}{\mathrm{d}r}\log(\tilde{w}_{\max})\right\}.$$

As is shown in Figure 5a, α_r decreases with increasing radial position, which means that the critical minimum step size increases. This can also be observed from the curves of Figure 5b. In this figure the growth rates from original PSEs for two different step sizes, $\Delta r = 10$ and 5 are given. As is shown there, only $\Delta r = 10$ gave a smooth solution through the whole computational domain. The growth rates for the step sizes $\Delta r = 1$ and $0{\cdot}1$ were also calculated from the original PSEs. However, these curves started to deviate so early from those in Figure 5b that we did not consider it meaningful to plot these in the same figure.

Here, as in the previous cases, when the modified PSEs were used, the numerical instability was removed. The results for $s = 20$ are given in Figure 5c. Equation (34) gave the critical value of s as $s = 7{\cdot}6$. The results for all step sizes used here collapsed to that of $\Delta r = 10$ from original PSEs.

Li and Malik [24] showed that, by dropping $\partial \tilde{p}/\partial r$ in the primitive-variable formulation, the step-size restriction could be relaxed. Using the vorticity–velocity formulation and dropping $\mathrm{d}\alpha/\mathrm{d}r$, they found that the step-size problem was relaxed further. They presented smooth results for $\Delta r = 1{\cdot}5$. However, by dropping $\partial \tilde{p}/\partial r$ or $\mathrm{d}\alpha/\mathrm{d}r$ the results became slightly different (see Figure 8 in Li and Malik [24]). Furthermore, by modifying the iteration method for α in vorticity–velocity formulation, they could reduce the step size to $\Delta r = 1$ and still obtain a numerically stable solution. Note that this value is still an order of magnitude larger than the smallest step size used in the calculations presented in Figure 5c.

It should be mentioned that the term $\mathrm{d}\alpha/\mathrm{d}r$ is not present in the equations used here. This follows naturally from the assumptions discussed in Section 2.2.

7. Discussion and conclusions

Comparing fundamental solutions of the spatially formulated linearized two-dimensional Navier-Stokes equations and the PSEs with constant coefficients, we have shown that the parabolizing procedure eliminates the most dangerous upstream propagating eigenmode. The remaining ellipticity makes the PSEs ill-posed, although a large streamwise step size can stabilize the numerical solution procedure.

In two-dimensional incompressible flows it is possible to apply the PSE-approximation on the stream-function-formulated equation, instead of the primitive-variable equations. It is shown here that this formulation is well-posed, which indicates why the step-size problem has been less severe than for other formulations. However, this formulation does not remove the numerical instability of PSE.

It was also shown that the parabolized stability equations can be modified such that the numerical instability is removed but the physical solution remains unaffected. This was done by the addition of a term proportional to the truncation error of the first-order backward Euler scheme, $s\mathcal{L}\tilde{\mathbf{q}}_x$. We pointed out that $\mathcal{L}\tilde{\mathbf{q}}_x$ is of $O(R^{-2})$. Thus, if s is of $O(1)$, this added term is as small as those which were neglected when the PSE-approximation was applied to the Navier-Stokes equations. Note especially that s need not be of $O(\Delta x)$. This procedure leads to well-posed equations, and to an elimination of the step-size restriction. It was possible to solve the PSEs for several different flows, with a marching step size considerably below the step-size restriction given by Li and Malik [23, 24]. It was also possible to derive a distinct step-size restriction for the stabilized equations. This became $\Delta x > 1/|\alpha_r| - 2s$, which implies that the step-size restriction is removed if $s > 0{\cdot}5/|\alpha_r|$. The simplicity of the implementation of the method discussed here should also be emphasized.

Appendix A. The method of multiple scales

The method of multiple scales is the foundation on which the PSE-method rests. For a presentation of the method of multiple scales see, for example, Nayfeh [26, 228–307]. Here, this method is applied to the disturbance equations. We start with Equations (10) in Section 3. In order to get a simple system, with the streamwise variation of the mean flow included, we assume $V = 0$ but $U_x \neq 0$. Under these conditions, the system of Equations (10) simplifies to

$$\frac{\partial \hat{\mathbf{q}}}{\partial x} = \mathcal{A}\hat{\mathbf{q}}, \qquad \mathcal{A} = \begin{bmatrix} 0 & -i\eta & 0 & 0 \\ 0 & 0 & 1 & 0 \\ 0 & -i\omega R + \eta^2 & UR & i\eta R \\ i\omega - \dfrac{\eta^2}{R} - U_x & i\eta U & -i\dfrac{\eta}{R} & 0 \end{bmatrix}. \tag{A1}$$

The basic assumptions in the multiple-scales method is that the solution can be divided into a slowly varying amplitude function and an exponential function

$$\hat{\mathbf{q}}(x) = \tilde{\mathbf{q}}(\xi)\, \mathrm{e}^{\frac{1}{\epsilon}\int_{\xi_0}^{\xi} \alpha(\zeta)\, \mathrm{d}\zeta}, \tag{A2}$$

where $\xi = \epsilon x$ and $\epsilon \ll 1$. Note that both the amplitude function $\tilde{\mathbf{q}}$ and the exponent α are slowly varying. A series expansions in ϵ is now introduced,

$$\tilde{\mathbf{q}}(\xi) = \sum_{n=0}^{\infty} \epsilon^n \tilde{\mathbf{q}}_n(\xi), \qquad \alpha(\xi) = \sum_{n=0}^{\infty} \epsilon^n \alpha_n(\xi). \tag{A3}$$

Also the matrix operator $\mathcal{A}(x)$ is assumed to be slowly varying in x,

$$\mathcal{A}(x) = \sum_{n=0}^{N} \epsilon^n \mathcal{A}_n(\xi). \tag{A4}$$

Since $(\partial/\partial x) = \epsilon(\partial/\partial\xi)$, $\mathcal{A}_0$ does not contain any streamwise derivatives of the mean flow; $\mathcal{A}_1$ contains only the first-order derivatives and so on. Introducing the assumption (A2) into Equation (A1) gives

$$\epsilon \frac{\partial \tilde{\mathbf{q}}}{\partial \xi} + \alpha \tilde{\mathbf{q}} = \mathcal{A}\tilde{\mathbf{q}}. \tag{A5}$$

If we introduce the expansions for $\tilde{\mathbf{q}}$, α and $\mathcal{A}$, and collect terms of the same order we find

$$\epsilon^0\text{:}\ (\mathcal{A}_0 - I\alpha_0)\tilde{\mathbf{q}}_0 = 0, \tag{A6a}$$

$$\epsilon^1\text{:}\ \frac{\partial \tilde{\mathbf{q}}_0}{\partial \xi} + \alpha_0 \tilde{\mathbf{q}}_1 + \alpha_1 \tilde{\mathbf{q}}_0 = \mathcal{A}_0 \tilde{\mathbf{q}}_1 + \mathcal{A}_1 \tilde{\mathbf{q}}_0, \tag{A6b}$$

$$\epsilon^2\text{:}\ \cdots. \tag{A6c}$$

The zeroth order equation shows that α_0 and $\tilde{\mathbf{q}}_0$ corresponds to one of the eigenvalues and eigenvectors of $\mathcal{A}_0$, respectively. The first-order equation can subsequently be used to obtain α_1 and $\tilde{\mathbf{q}}_1$, and so on, to obtain as many terms as are needed.

Note that $\mathcal{A}_0$ is the same matrix as the one appearing in Section 3.1, but with α and V equal to zero. Thus, the eigenvalues and right-hand eigenvectors to $\mathcal{A}_0$ can also be found from Equations (13) and (14). Let us introduce the left-hand eigenvectors of $\mathcal{A}_0$ defined by

$$\Psi_i^T \mathcal{A}_0 = \lambda_i \Psi_i^T .$$

Since the operator $\mathcal{A}_0$ has distinct eigenvalues, the left and right eigenvectors corresponding to different eigenvalues are orthogonal, $\Psi_i \cdot \Phi_j = 0$ if $i \neq j$. Here

$$\Psi_1 = \left(i\omega R - \eta^2,\ iUR\frac{\lambda_1^2}{\eta},\ -i\frac{\lambda_1^2}{\eta},\ \lambda_1 R \right)^T , \tag{A7a}$$

$$\Psi_2 = \left(i\omega R - \eta^2,\ iUR\frac{\lambda_2^2}{\eta},\ -i\frac{\lambda_2^2}{\eta},\ \lambda_2 R \right)^T , \tag{A7b}$$

$$\Psi_3 = (i\eta[i\omega R - \eta^2],\ -i\omega R\lambda_3,\ \lambda_3^2,\ i\eta R\lambda_3)^T , \tag{A7c}$$

$$\Psi_4 = (i\eta[i\omega R - \eta^2],\ -i\omega R\lambda_4,\ \lambda_4^2,\ i\eta R\lambda_4)^T . \tag{A7d}$$

In order to solve for $\tilde{\mathbf{q}}_1$ in the first-order equations we expand the solution in the right-hand eigenvectors of $\mathcal{A}_0$,

$$\tilde{\mathbf{q}}_1 = c_1\Phi_1 + c_2\Phi_2 + c_3\Phi_3 + c_4\Phi_4. \tag{A8}$$

Introducing the above expression into (A6b) we have

$$\left(\frac{\partial \tilde{\mathbf{q}}_0}{\partial \xi} - \mathcal{A}_1 \tilde{\mathbf{q}}_0 \right) + \sum_{i=1}^{4} c_i(\alpha_0 - \lambda_i)\Phi_i + \alpha_1 \hat{\mathbf{q}}_0 = 0. \tag{A9}$$

Replacing $\hat{\mathbf{q}}_0 = \Phi_4$ and $\alpha_0 = \lambda_4$ (here Φ_4 is the relevant physical solution) and taking the dot-product with the three first left-hand-side eigenvectors we have

$$c_i = (\Psi_i \cdot \Phi_i)^{-1}(\lambda_i - \lambda_4)^{-1}\Psi_i \cdot \left(\frac{\partial \Phi_4}{\partial \xi} - \mathcal{A}_1\Phi_4 \right); \quad i = 1, 2, 3. \tag{A10}$$

Taking the dot-product of (A9) with Ψ_4 we obtain an equation for the first-order term in the expansion for α,

$$\alpha_1 = (\Psi_4 \cdot \Phi_4)^{-1}\Psi_4 \cdot \left(\mathcal{A}_1\Phi_4 - \frac{\partial \Phi_4}{\partial \xi} \right). \tag{A11}$$

The first term in the expansion for the amplitude function must be linearly independent from the other terms; thus c_4 must be equal to zero in all terms but the first. The first-order amplitude function, $\tilde{\mathbf{q}}_1$, can be calculated from the coefficients c_1, c_2, c_3 and α_1.

Appendix B. Equations governing the rotating-disk flow

The PSEs, based on the same approximations used in Section 2.2, that govern the disturbances in a rotating-disk flow are

$$\tilde{u}_r + \left[i\alpha + \frac{1}{r} \right] \tilde{u} + \tilde{v}_y + i\frac{n}{r}\tilde{w} = 0, \tag{B1a}$$

$$\begin{aligned} &UR\tilde{u}_r + R\tilde{p}_r + \left[i\alpha UR + i\frac{R}{r}nW - i\omega R + \frac{n^2}{r^2} + RU_{ry} - 3i\frac{\alpha}{r} + \frac{3}{r^2} + 3\alpha^2 \right] \tilde{u} \\ &\quad + RU_y\tilde{v} + \left[4i\frac{n}{r^2} + 2 + 2\frac{\alpha n}{r} - 2R\frac{W}{r} \right] \tilde{w} \\ &\quad + i\alpha R\tilde{p} + VR\tilde{u}_y - 2i\alpha\tilde{v}_y - \tilde{v}_{yy} = 0, \end{aligned} \tag{B1b}$$

$$\begin{aligned} &UR\tilde{v}_r + \left[i\alpha UR + i\frac{R}{r}nW - i\omega R + \frac{n^2}{r^2} + RV_y - i\frac{\alpha}{r} + \alpha^2 \right] \tilde{v} \\ &\quad - \left[2i\alpha + \frac{2}{r} \right] \tilde{u}_y + VR\tilde{v}_y - 2i\frac{n}{r}\tilde{w}_y + R\tilde{p}_y - 3\tilde{v}_{yy} = 0, \end{aligned} \tag{B1c}$$

$$\begin{aligned} &UR\tilde{w}_r + \left[R\frac{W}{r} + RW_{ry} + 2\frac{\alpha n}{r} - 4i\frac{n}{r^2} - 2 \right] \tilde{u} + RW_y\tilde{v} \\ &\quad + \left[i\alpha UR + i\frac{R}{r}nW - i\omega R + 3\frac{n^2}{r^2} + \frac{UR}{r} - i\frac{\alpha}{r} + \alpha^2 + \frac{1}{r^2} \right] \tilde{w} \\ &\quad - iR\frac{n}{r}\tilde{p} - 2i\frac{n}{r}\tilde{v}_y + VR\tilde{w}_y - \tilde{w}_{yy} = 0, \end{aligned} \tag{B1d}$$

with boundary conditions

$$\tilde{u} = \tilde{v} = \tilde{w} = 0, \quad y = 0 \quad \text{and} \quad y = \infty.$$

Here $\tilde{u}$, $\tilde{v}$, and $\tilde{w}$ are the non-dimensional disturbance velocity components in the r, y and θ directions, respectively, and $\tilde{p}$ represent the disturbance pressure.

Acknowledgment

We acknowledge funding by the Swedish National Board for Industrial and Technical Development (NUTEK). The first author wishes to thank Gunilla Kreiss for introducing him to the concept of well-posedness.

References

1. M. Gaster, On the effects of boundary-layer growth on flow stability. *J. Fluid Mech.* 66 (1974) 465–480.
2. W. S. Saric and A. H. Nayfeh, Non-parallel stability of boundary-layer flows. *Phys. Fluids* 18 (1975) 945–950.
3. S. A. Gaponov, The influence of flow non-parallelism on disturbance development in the supersonic boundary layers. In: *Proc. 8th Canadian Congr. of Appl. Mech.* (1981) pp. 673–674.
4. N. M. El-Hady, Nonparallel instability of supersonic and hypersonic boundary layers. *Phys. Fluids A* 3 (1991) 2164–2178.
5. P. Hall, The linear development of Görtler vortices in growing boundary layers. *J. Fluid Mech.* 130 (1983) 41–58.
6. N. Itoh, The origin and subsequent development in space of Tollmien-Schlichting waves in a boundary layer. *Fluid Dyn. Res.* 1 (1986) 119–130.
7. Th. Herbert and F. P. Bertolotti, Stability analysis of nonparallel boundary layers. *Bull. Am. Phys. Soc.* 32 (1987) 2079.
8. Th. Herbert, Boundary-layer transition – analysis and prediction revisited. *AIAA* Paper 91-0737 (1991).
9. F. P. Bertolotti, *Linear and Nonlinear Stability of Boundary Layers with Streamwise Varying Properties.* Ph.D. Thesis. The Ohio State University (1991) 189 pp.
10. F. P. Bertolotti, Th. Herbert and S. P. Spalart, Linear and nonlinear stability of the Blasius boundary layer. *J. Fluid Mech.* 242 (1992) 441–474.
11. M. Simen, Local and nonlocal stability theory of spatially varying flows. In: M. Y. Hussaini, A. Kumar and C. L. Streett (eds), *Instability, Transition and Turbulence*, New York: Springer-Verlag (1992) pp. 181–201.
12. M. Simen, *Lokale und nichtlokale Instabilität hypersonischer Grenzschichtströmungen.* Ph.D. Thesis. DLR FB 93-31 (1993) 200 pp.
13. S. G. Rubin, A Review of marching procedures for parabolized Navier-Stokes equations. In: T. Cebeci (ed.), *Proc. Symp. Num. and Phys. Aspects Aerodyn. Flows*. New York: Springer-Verlag (1981) pp. 171–186.
14. S. G. Rubin and J. C. Tannehill, Parabolized/reduced Navier-Stokes computational techniques. *Ann. Rev. Fluid Mech.* 24 (1992) 117–144.
15. D. A. Anderson, J. C. Tannehill and R. H. Pletcher, *Computational Fluid Mechanics and Heat Transfer*. New York: Hemisphere (1984) 599 pp.
16. S. C. Lubard and W. S. Helliwell, Calculation of the flow on a cone at high angle of attack. *AIAA J.* 12 (1974) 965–974.
17. Y. C. Vigneron, J. V. Rakish and J. C. Tannehill, Calculation of supersonic viscous flow over delta wings with sharp subsonic leading edges. *AIAA* Paper 78-1137 (1978).
18. Y. C. Vigneron, J. V. Rakish and J. C. Tannehill, Calculation of supersonic viscous flow over delta wings with sharp subsonic leading edges. *NASA TM*-78500 (1978).
19. T. C. Lin and S. G. Rubin, A numerical model for supersonic viscous flow over a slender reentry vehicle. *AIAA* Paper 79-0205 (1979).
20. S. G. Rubin and A. Lin, Marching with the parabolized Navier-Stokes equations. *Isr. J. Technol.* 18 (1980) 21–31.
21. M. Israeli and A. Lin, Iterative numerical solutions and boundary conditions for the parabolized Navier-Stokes equations. *Comput. Fluids* 13 (1985) 397–409.
22. H. Haj-Hariri, Characteristics analysis of the parabolized stability equations. *Stud. Appl. Math.* 92 (1994) 41–53.
23. F. Li and M. R. Malik, Mathematical nature of parabolized stability equations. In: R. Kobayashi (ed.), *Laminar-Turbulent Transition. Proc. 4th IUTAM Symposium Sendai/Japan 1994*. Berlin: Springer-Verlag (1995) pp. 205–212.
24. F. Li and M. R. Malik, On the nature of PSE approximation. *Theor. Comp. Fluid Dyn.* 8 (1996) 253–273.
25. H.-O. Kreiss and J. Lorenz, *Initial-Boundary Value Problems and the Navier-Stokes Equations*. New-York: Academic Press (1989) 402 pp.
26. A. Nayfeh, *Perturbation Methods*. New-York: John Wiley & Sons (1973) 425 pp.